Reaction cross sections for $^{16}O + ^{12}C$

J. J. Kolata
University of Notre Dame, Notre Dame, Indiana 46556

R. M. Freeman, F. Haas, B. Heusch, and A. Gallmann
Centre de Recherches Nucleaires, 67037 Strasbourg, France

(Received 5 July 1978)

The partial production cross sections for 11 nuclides produced in the fusion of $^{12}C + ^{16}O$, in the energy region from 17–28 MeV (c.m.), have been measured and compared to an evaporation-model calculation. The comparison, though not completely satisfactory, provides no evidence that such models are inadequate to explain the observations. The "effective" α-particle evaporation yield, deduced from measured partial production cross sections, is shown to be in excellent agreement with previously measured α-particle yields up to 26 MeV (c.m.). The implications of this agreement for the apparent discrepancies between heavy-particle and γ-ray measurements of the fusion yield are discussed. The average total fusion yield, including 3α evaporation to ^{16}O, is found to be nearly constant at about 1 barn from 20–26 MeV (c.m.). Narrow, regular fluctuations in the yield, with a periodicity of 725 keV and an average width of 150–200 keV are observed. These anomalies are correlated in the various partial-production excitation functions. It is found, however, that the ^{16}O and ^{20}Ne excitation functions are anticorrelated and possible explanations for this latter observation are discussed.

[NUCLEAR REACTIONS Complete fusion, $^{12}C + ^{16}O$, $E_{c.m.} = 17–28$ MeV; evaporation model analysis of nuclide distributions: correlation analysis of fluctuations.]

I. INTRODUCTION

The subject of resonant phenomena and intermediate structure in heavy-ion reactions has been of intense interest lately, with important new data appearing in the literature almost monthly. (For a small sampling of recent work in this field, see Refs. 1–4 and references therein.) The present experiment was motivated by the discovery,[5] two years ago, of unexpected structure in the complete fusion cross section for the interaction of ^{16}O with ^{12}C, and the suggested correlation of these data with pronounced fluctuations in back-angle elastic scattering for this system.[6] Some of the results of this work, dealing primarily with the gross structure of the fusion excitation function, have already been published,[7] and we shall here concentrate on a more complete discussion of the experimental technique, an evaporation-model calculation of the nuclide distributions, and a fluctuation analysis of the observed fine structure. The intriguing possibilities suggested by the observed regular correlations in the latter analysis will be examined in some detail.

II. EXPERIMENTAL METHOD

The experiment was performed with 40–65 MeV ^{16}O beams from the Strasbourg MP-tandem accelerator. Great care was taken to ensure accurate relative normalization of the data, which is of major importance in excitation-function experiments. The 2-mm diam. beam-defining collimator and subsequent 3-mm anti-scattering apertures (Fig. 1) were insulated from the beam line and biased at + 300 *V* relative to local ground (the target chamber) in order to suppress streaming of electrons from their edges. In addition, strong permanent magnets were placed above and below the beam for further electron suppression. The targets were surrounded by a liquid-nitrogen-cooled shroud (Fig. 1), with a 1-cm diam. entrance aperture, to reduce carbon buildup. This shroud was electrically connected to the target, and both were maintained at + 300 V relative to the chamber to insure complete charge collection. Finally, the beam current striking the collimator was minimized, and any experimental run in which a substantial departure from this minimum occurred was repeated. With all of these precautions, it was found that the relative normalizations derived from charge collection agreed to within better than ± 2% with those determined from Coulomb excitation of the Au target backing. Moreover, the internal error computed from the observed scatter of repeated observations suggests that the actual uncertainty in the Coulomb-excitation values (our primary normalization) is less than ± 0.5%. Note that, for the purposes of this experiment, one only requires that the Au Coulex cross section display

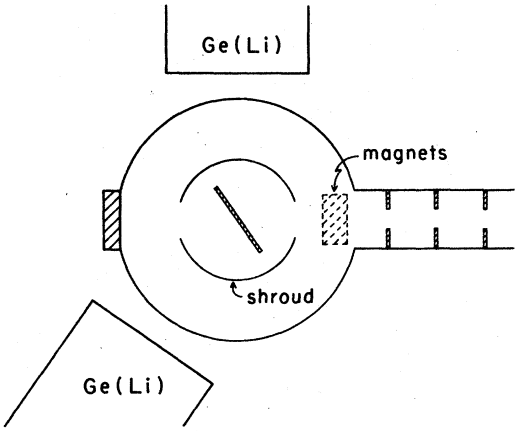

FIG. 1. Schematic diagram of the target chamber. The location of all elements, including the Ge(Li) detectore, is approximately to scale.

locally smooth behavior. The long-range trend of the data is then determined from charge normalization. However, we have also compared the measured Coulex cross sections to the predictions of a thick-target Winther-deBoer multiple Coulomb excitation program, obtained from Dr. R. O. Sayer of the Oak Ridge National Laboratory. The observed long-range behavior is well reproduced up to the highest energy used in this experiment (which is still well below the Coulomb barrier for O on Au).

As mentioned above, the target for this experiment was deposited onto a thick, high-Z, metallic backing. The ^{12}C target typically consisted of 45 $\mu g/cm^2$ of natural C evaporated onto Au, oriented at 35° relative to the beam direction and surrounded by a liquid-nitrogen-cooled shroud to eliminate C buildup (Fig. 1). The analysis of repeated measurements made at wide intervals during the course of the experiment indicated reproducibility of the results to within ± 0.5%, so that the effect of C buildup was, in fact, negligible. This conclusion was confirmed by the observation that spectra taken with an ^{16}O beam incident on the Au backing at the end of the experimental runs showed no evidence of γ rays due to $^{16}O + ^{12}C$ reactions.

Reaction γ rays, up to 6 MeV in energy, were detected by two Ge(Li) detectors of >15% efficiency at 90° and 55° to the incident beam (Fig. 1). A typical spectrum taken at 90° is shown in Fig. 2. The sharp γ-ray lines in this illustration correspond to the decay of relatively long-lived ($\tau \gtrsim 2$ ps) states in the residual nuclei indicated (see Table I). The peaks due to the other γ rays are Doppler broadened. The identification of each of these transitions with a particular residual nucleus was facilitated by the availability of tabulations of expected and observed transitions in this mass region.[8,9]

Excitation functions for the production of various nuclides in the evaporation chain were determined from the areas of the appropriate γ-ray lines, indicated by asterisks in Fig. 2.[7] These constitute all known ground-state (gs) transitions between 300 keV and 6 MeV in nuclei in this mass region which were also observed in the present experiment. Several known gs transitions which were not observed, presumably because they were too weak, are listed in Table I of Ref. 7. The relative efficiencies of the γ-ray detectors determined with ^{56}Co and ^{152}Eu sources, and the absolute efficiencies determined with calibrated sources of ^{137}Cs, ^{88}Y, and ^{60}Co, are shown in Fig. 3.

The efficiency-corrected areas, together with the known mixing ratios[10] for the transitions involved, were used to obtain angle-integrated γ-ray yields at each energy. Since the overwhelming majority of the observed γ rays correspond to quadrupole or dipole transitions, measurements at three angles are sufficient to uniquely determine the γ-ray angular distribution. We can reduce this requirement to only two measurements by invoking the empirical relationship[11] between the coefficients of the P_2 and P_4 terms of angular distributions appropriate to transitions from highly aligned states. Since all measured P_2 coefficients are consistent with strong alignment, errors in the computed cross sections arising from uncertainties in the γ-ray angular distributions are estimated at $\lesssim 2\%$.

The absolute normalization of the experimental excitation functions was determined from the yield of 1634-keV γ rays from the $^{16}O + ^{12}C$ reaction, using a self-supporting C foil of known areal density (measured with an α-particle thickness gauge). For this experiment the plug at the rear of target chamber (Fig. 1) was removed and the beam current was measured in a large Faraday cup at a distance from the target. Care was taken to eliminate possible systematic error due to electrons striking the Faraday cup and/or to multiple scattering of ^{16}O ions out of the beam. Measurements made at 45, 55, 60, and 65 MeV incident energy agreed to within ± 4% after correcting for the relative cross sections and the differing average charge states of the beam after traversing the target. The total estimated uncertainty of ± 7% is dominated by the uncertainty in target thickness.

III. RESULTS AND DISCUSSION

The yields of eleven nuclides in the evaporation chain from the ^{28}Si compound nucleus were de-

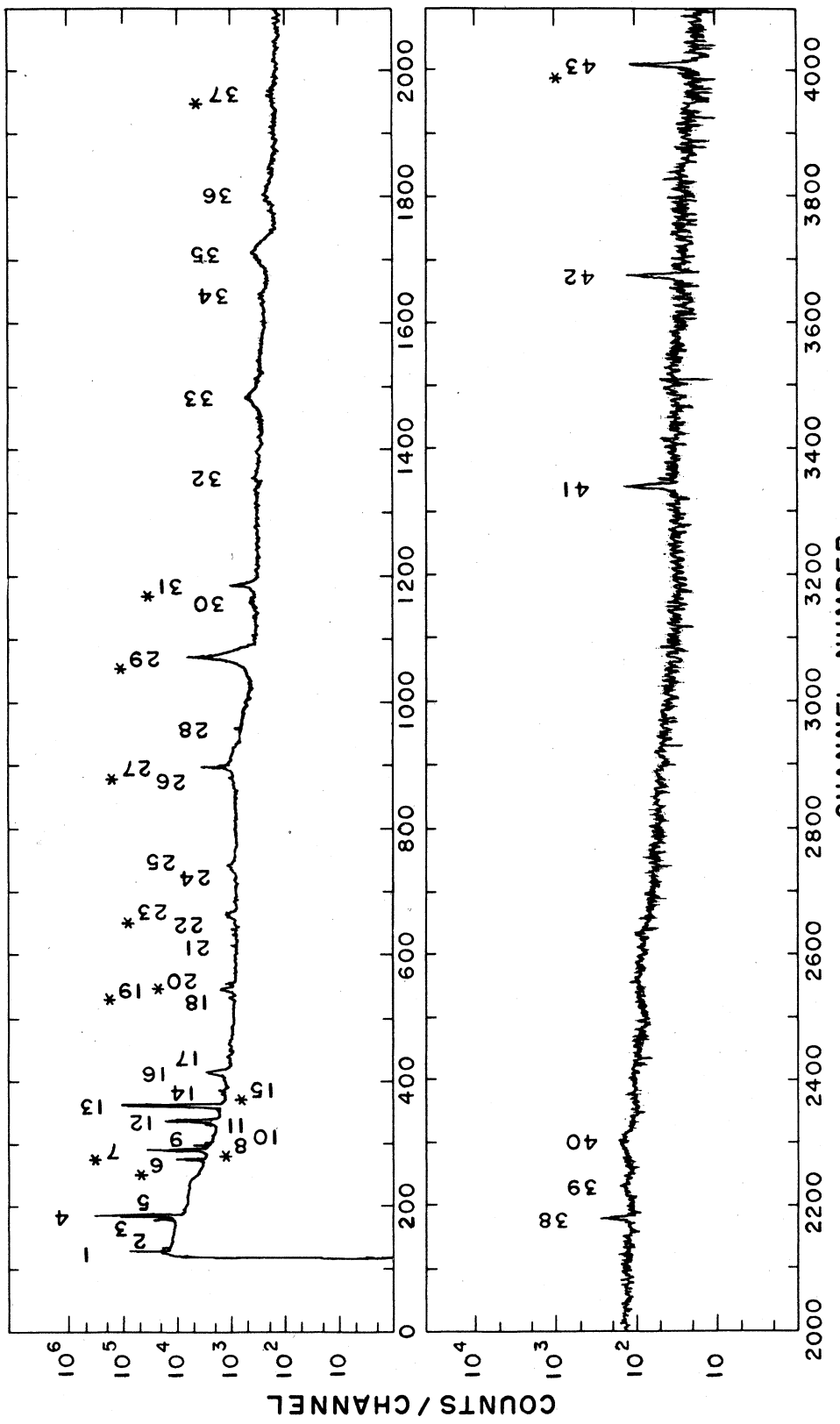

FIG. 2. Typical γ-ray spectrum, for $^{12}C(^{16}O, x)$ at $E_{lab}=40$ MeV. Lines identified with an asterisk were used to determine the various nuclide production cross sections.

TABLE I. Key for the γ-ray lines labeled in Fig. 2.

Peak No.	E_γ (keV)	Identification	Peak No.	E_γ (keV)	Identification
1	192	Au	23	1015	^{27}Al
2	202	Au	24	1123	^{20}Ne(1634)SE
3	269	Au	25	1130	^{26}Mg
4	279	Au	26	1342	^{26}Al
5	296	^{26}Al	27	1369	^{24}Mg
6	417	^{26}Al	28	1461	^{40}K(β^-)
7	440	^{23}Na	29	1634	^{20}Ne
8	451	^{23}Mg	30	1772	^{23}Na
9	459	Au	31	1809	^{26}Mg
10	476	^{26}Al	32	2076	^{23}Na
11	505	Au	33	2264	^{23}Na
12	511	m_0c^2	34	2511	^{26}Mg
13	547	Au	35	2613	^{20}Ne
14	576	Au	36	2754	^{24}Mg
15	585	^{23}Mg	37	3004	^{27}Al
16	628	^{23}Na	38	3334	^{20}Ne
17	691	Ge	39	3413	^{23}Na
18	812	Au	40	3519	^{24}Mg
19	830	^{26}Al	41	5108	^{16}O(6130)DE
20	844	^{27}Al	42	5619	^{16}O(6130)SE
21	937	Au	43	6130	^{16}O
22	1003	^{26}Mg			

termined according to the methods discussed in the preceding section.[12] Excitation functions for the formation of ^{23,25,26}Mg and ^{26,27}Al are shown in Fig. 4, and the yields of ^{16}O (3$^-$) and ^{20}Ne appear in Fig. 5. Of the remaining nuclides, data on the production of ^{24}Mg and ^{23}Na (as well as the total fusion yield) have been given in Ref. 7, and the excitation functions for ^{22}Ne and ^{22}Na are incomplete since these systems are appreciably formed only at the highest energies studied.

Subsequent to the publication of Ref. 7, the results of two similar γ-ray measurements[13,14] have appeared in print. The agreement amongst these experiments in their respective regions of overlap is uniformly excellent, although only relative cross sections from Ref. 13 can be compared since absolute yields were not determined in that work. Also, another heavy-particle-

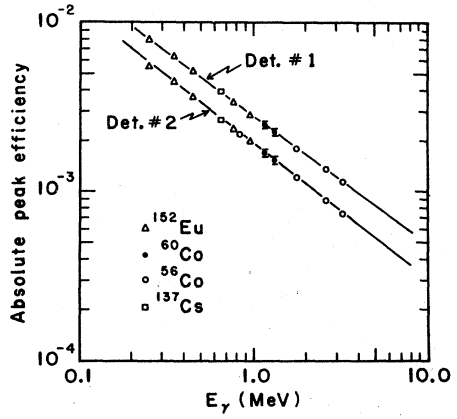

FIG. 3. Absolute peak efficiencies of the Ge(Li) detectors, as determined with several sources. Detector #1 was placed at 90° to the beam.

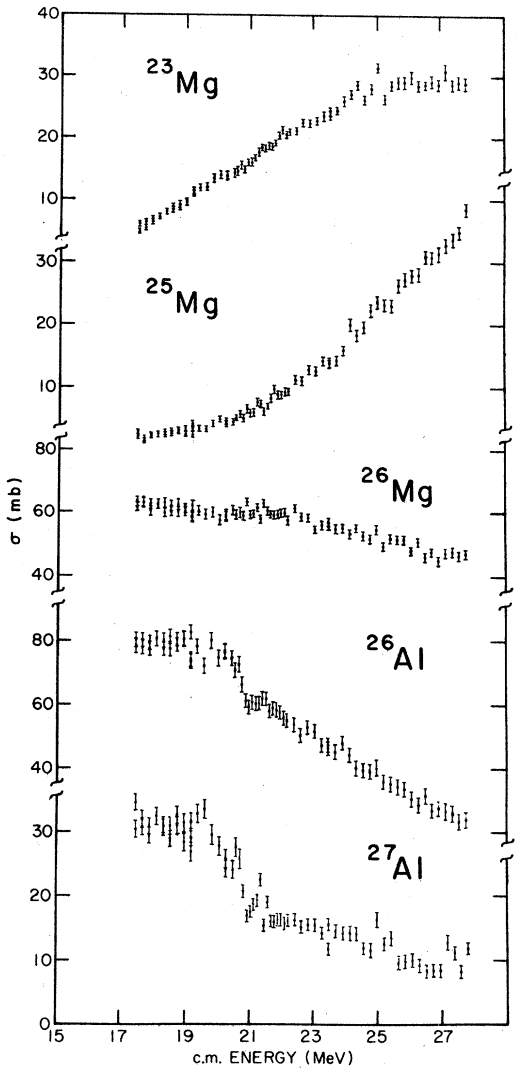

FIG. 4. Excitation functions for the production of ^{23,25,26}Mg and ^{26,27}Al from ^{12}C(^{16}O, x).

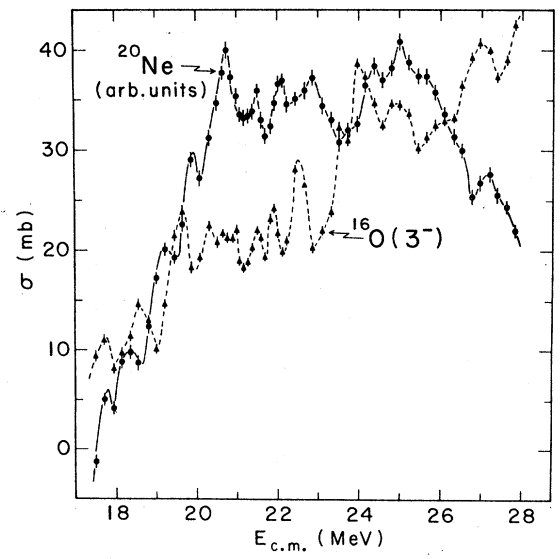

FIG. 5. Excitation functions for the production of ^{20}Ne and ^{16}O(3$^-$) from ^{12}C (^{16}O, x). The ^{20}Ne data are plotted on an arbitrary scale with suppressed zero for comparison purposes. (See Ref. 7 for the absolute cross section plot). The dashed and solid lines are drawn to guide the eye, and have no further theoretical significance.

detection experiment[15] on this system, in addition to that of Weidinger *et al.*,[16] has recently been performed. In this regard, it is interesting to reinvestigate the question of the apparent anomalous yield of ^{20}Ne first discussed in Ref. 7. In brief, the formation of ^{20}Ne, signaled by the 1634-keV γ ray from its first excited state, was found to be substantially more probable than suggested by the data of Ref. 16 (500 mb vs 257 mb at a c.m. energy of 26 MeV). On the other hand, agreement between the independent results of Refs. 7 and 14 at their overlap energy [18 MeV (c.m.)] confirmed the absolute cross section scale, so the discrepancy can only be due to a problem common to both γ-ray experiments. One possibility, already discussed in Ref. 7, is that the unresolved (and Doppler broadened) 1636.5-keV line from the 2076-keV state in ^{23}Na is contributing to the observed intensity of the 1634-keV γ ray. The magnitude of this contamination can be determined from the 8% ground-state branch of this level at 2076.3 keV, which appears very weakly in Fig. 2. The estimated upper limit is ~10% of the total intensity of the ^{20}Ne line, which is insufficient to completely resolve the discrepancy. Nevertheless, it is also clear from Fig. 2 that the contamination is likely to be near this upper limit, since the 629-keV line originates in a transition that feeds the 2076-keV level. From its intensity, we can estimate that about 8–10% of the "1634-keV" γ ray is actually due to ^{23}Na. Furthermore, the most recent particle-detection experiment (Ref. 15) has found a ^{20}Ne production cross section of 310 mb at 26.6 MeV (c.m.) so that the magnitude of the discrepancy has been reduced from over 50% to only 30%. Some of the remaining discrepancy is undoubtedly due to the fact that the ^{20}Ne yield decreases quite rapidly between 26 and 27 MeV (c.m.) (see Fig. 5). It would thus be of some interest to repeat both types of experiment at a single laboratory using the same target, to attempt to resolve the remaining differences.

Actually, Ref. 15 contains additional useful reaction data, in that the α-particle production cross section was also measured. We have converted our measured nuclide yields to an effective

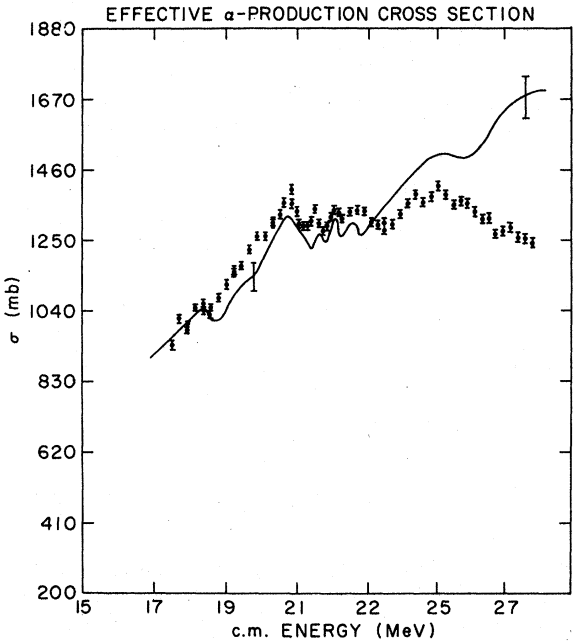

FIG. 6. Effective α-particle-production excitation function deduced from the nuclide distributions. The solid line is drawn through the data of Ref. 15, with two representative error bars.

α-particle production cross section $\sigma_\alpha^{\text{eff}}$ under the assumption that ^{23,24}Mg and ^{23}Na are each associated with the evaporation of a single α particle, and that ^{20}Ne results from (2α) emission. The values determined this way are compared to the measured α-particle production cross section in Fig. 6 (where the solid curve is a representation of the results of Ref. 15). It can be seen that the agreement is very good up to $E_{c.m.} \simeq 22$ MeV, particularly if our $\sigma_\alpha^{\text{eff}}$ values are reduced by about 80–100 mb to account for the reduction in ^{20}Ne cross section discussed above. The effective proton yields can also be compared to data presented in Ref. 15. The deduced excitation function is structureless and slowly rising from 17–27 MeV (c.m.), in excellent agreement with the results of Ref. 15. The absolute magnitude of σ_p^{eff} is everywhere ~10% less than that shown in Ref. 15 (i.e., within the mutual experimental errors of the two measurements). It is interesting to note that $\sigma_\alpha^{\text{eff}}$ and the measured α-particle production cross section track each other very well below 19 MeV (c.m.), a region in which there is marked *disagreement* between the γ-ray measurements (Refs. 7, 13, 14) on one hand, and the particle detection data (Ref. 5) on the other hand, as to the gross structure of the total fusion excitation function. This observation places severe constraints on possible mechanisms which can be invoked to explain the latter disagreement. For example, direct (2α) evaporation to the ground state of ^{20}Ne is ruled out since this mechanism would be reflected in the total α-particle yield.

As discussed in Ref. 15, the rapid increase in σ_α beyond 22 MeV (c.m.) can be attributed to the onset of 3α evaporation to ^{16}O. In the present experiment, we have a measure of the probability for this process in the ^{16}O (3^-) excitation function of Fig. 5. The evaporation-model calculations (see below) suggest that most of this cross section is due to 3α evaporation, at least above 20 MeV (c.m.). Converting this yield to an effective α production cross section and adding it to the results shown in Fig. 6, we find good agreement with the measured α-particle yield up to about 26 MeV (c.m.). (The apparent rapid increase in yield beyond this energy is not at present understood). The increasing yield of ^{16}O via (3α) evaporation accounts for the decrease in the measured fusion cross section beyond 25 MeV (c.m.) reported in Refs. 5 and 7, since such processes were excluded in these experiments. Apparently, the average fusion yield is essentially constant at about 1 barn over the energy interval from 20–26 MeV (c.m.).

IV. EVAPORATION-MODEL CALCULATIONS

The excitation functions for production of the various nuclides were compared to the predictions of Hauser-Feshbach theory using the Monte Carlo code LILITA.[17] The complexity of the successive evaporation process is such that several approximations must be made to achieve reasonable computation times. The first approximation is the use of a sharp cutoff model in the entrance channel, leading to a compound-nuclear spin distribution given by

$$P_J = \frac{2J+1}{(J_c+1)^2}, \tag{1}$$

where J_c is the critical angular momentum. In the present case, we use the J_c values of Malmin.[18,19] In principle, the reaction cross section is related to the critical angular momentum by

$$\sigma_r = \pi \lambda^2 (J_c+1)^2. \tag{2}$$

Owing to the fact that the experimental fusion yield is everywhere substantially smaller than the reaction cross section predicted by the optical model, as discussed in Ref. 7, we have chosen to normalize the predicted value of σ_r to the experimental data. The alternate procedure of deducing J_c from the experimental fusion cross section does not seem justified in view of the fact that the physical basis for the anomalously small fusion yield

is not understood.[20] In any event, the relative yields of the major reaction products are not critically sensitive to small (10%) changes in J_c.[21]

The level densities of the various nuclides were determined from a constant temperature approximation to the Fermi gas formula,[22] except for the low-excitation energy region of discrete levels where a uniform level density (computed from known levels) was used. The effective moment of inertia in the discrete spectrum was taken to be one half the rigid body value for $r_0 = 1.2$ fm.

The deexcitation of the compound nucleus proceeds by successive p, n, α, and γ emission. LILITA uses a Fermi-function parametrization of the particle transmission coefficients

$$T_l^{\alpha}(\epsilon) = \frac{C_{\alpha}}{1+\exp[(B_l-\epsilon)/\Delta B_l]}, \tag{3}$$

where B_l is the sum of the Coulomb plus centrifugal barriers and α denotes the particle type. The constants are chosen by comparison to optical-model transmission coefficients,[17] and were taken to be $\Delta = 0.08$, $C_{\alpha} = (0.8, 0.8, 1.0)$ for (n, p, α), respectively. However, T_l is arbitrarily set equal to zero if it is less than a cutoff value (taken here to be 10^{-3}). γ-ray competition is provided for in an approximate way by a parameter giving the average probability of γ decay in the discrete region, usually equal to about 0.01.

The experimental and calculated excitation functions are compared in Fig. 7. It can be seen that, while there are strong similarities between prediction and experiment (particularly for the ^{20}Ne, ^{23}Na, ^{26}Mg, and ^{16}O channels), the overall agreement cannot be considered satisfactory. In particular, the single-proton-emission and single-α-emission channels (^{27}Al and ^{24}Mg) seem to be "trapping flux" in the calculation at the expense of pn and 2α evaporation. While it is true that, at a given energy, one can improve the fit to the nuclide distribution by making modest changes in the level-density parameters for individual nuclei, the improvement does not carry over into an improved prediction for the excitation functions. Furthermore, comparison to similar calculations for the fusion of $^{16}O + ^{16}O$ shows conclusively that the problems are not associated with individual level-density parameters.[23] Finally, the predicted nuclide distributions at $E_{c.m.} = 26$ MeV do not match those of Weidinger *et al.*[16] although most of the parameters (including the level-density parameters) are the same.

We have traced the problem to the calculation of the particle transmission coefficients in LILITA. The trapping of flux can be reduced by taking a smaller value for the cutoff parameter (say 10^{-4} or 10^{-5} rather than 10^{-3}), but the predictions are inordinately sensitive to the exact cutoff value employed. Furthermore, the parametrization of Eq. (3) is too inflexible to allow good matching to the optical-model transmission coefficients at the level of 10^{-3}, much less at 10^{-4} or 10^{-5}. Thus, we conclude that further improvements to the predictions shown in Fig. 7 must await a more realistic method to calculate the light-particle transmission coefficients.

On the other hand, the calculation of details of the nuclide production cross sections (par-

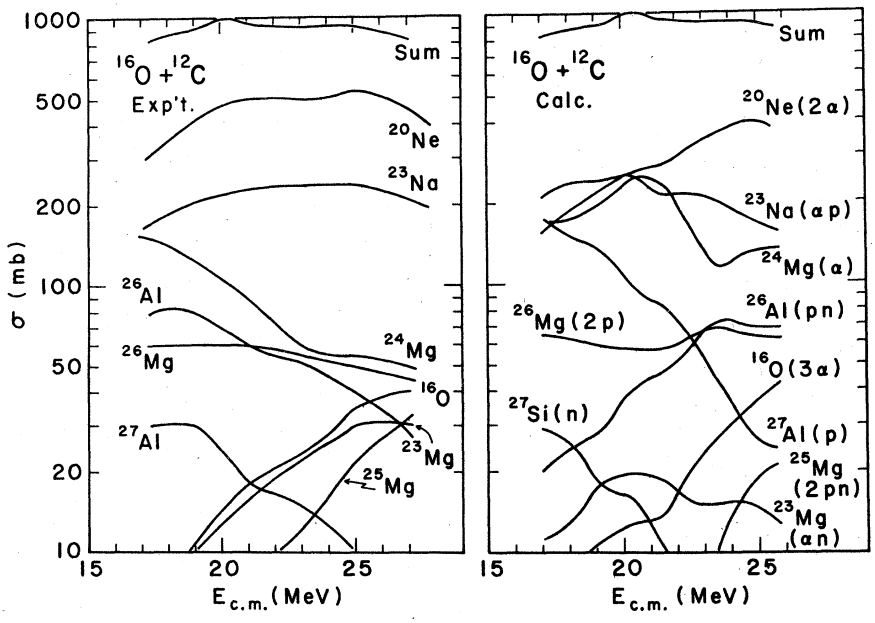

FIG. 7. Experimental and calculated average nuclide distributions.

ticularly if one requires the reproduction of excitation functions with fixed level-density parameters) represents a most severe test of the evaporation model. The results shown in Fig. 7 are remarkably good from this point of view. Certainly, there is no evidence from this experiment that standard statistical models are inadequate to predict the average behavior of the nuclide production cross sections in the $^{12}C + ^{16}O$ reaction.

V. CORRELATION ANALYSIS OF THE REACTION CROSS SECTIONS

Recently, Jachcinski *et al.*[24] have reported a striking correlation of broad resonances in the $^{12}C(^{16}O, ^{16}O)^{12}C^*$ (2^+, 4.44 MeV) reaction with similar structures in our fusion cross section data. They interpreted these correlations as evidence for the existence of shape resonances in the $^{12}C + ^{16}O$ system, and suggested that a comparison to other strong inelastic channels, such as $^{16}O^*$ (3^-), might also be interesting. This suggestion, together with our recent analysis of ^{16}O (3^-) data (Fig. 5), prompted the correlation analysis reported here. Correlated gross structure was indeed observed, but the behavior of fine structure in the data turned out to be even more striking and we will here concentrate on this aspect.

The analysis was performed using the computer codes AUTOCORR and CROSSCORR of Malmin.[18]

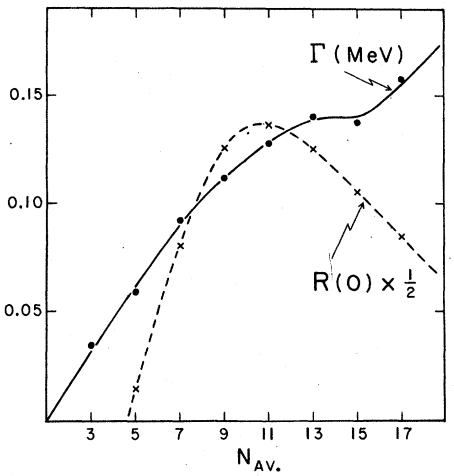

FIG. 8. Illustration of the method of choosing the optimum averaging interval. The coherence width Γ (corrected for the oscillations shown in Fig. 9) reaches a plateau for N_{av}=11–15. The absolute magnitude of the ^{16}O–^{20}Ne reduced cross correlation function reaches a peak at N_{av}=11. On the basis of these results, an averaging interval N_{av}=11 (corresponding to 1.18 MeV) was chosen.

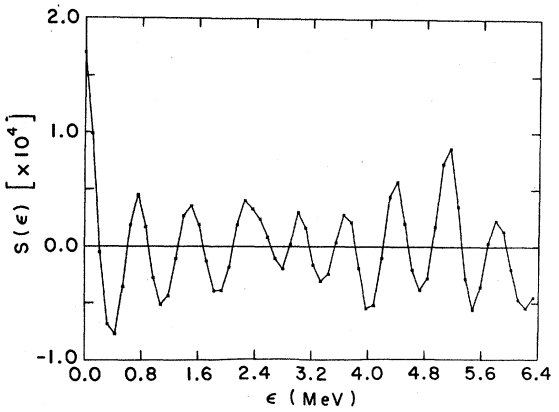

FIG. 9. Autocorrelation function $S(\epsilon)$ for the total fusion cross section data, using N_{av}=11. Note the regular oscillations, with a periodicity of 725 keV, which persist out to $\epsilon > 6$ MeV. Traces of the gross-structure modulation (Ref. 7) with a periodicity of ~2.25 MeV, are also visible.

We define the correlation function

$$S_{\alpha\alpha'}(\epsilon) = \left\langle \left[\frac{\sigma_\alpha(E)}{\langle\sigma_\alpha(E)\rangle} - 1\right]\left[\frac{\sigma_{\alpha'}(E+\epsilon)}{\langle\sigma_{\alpha'}(E+\epsilon)\rangle} - 1\right]\right\rangle, \quad (4)$$

where the energy-dependent average cross section is given by

$$\langle\sigma(E_i)\rangle_N = \frac{1}{N}\sum_{j=i-N/2}^{i+N/2}\sigma(E_j),$$

according to the method of Pappalardo.[25] The optimum averaging interval N must be determined[19,25] from the autocorrelation function $S_{\alpha\alpha}(E)$.

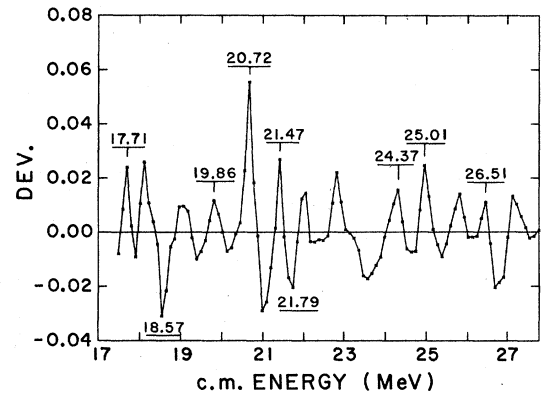

FIG. 10. Deviations of the total fusion cross section from the local average. The strongly anomalous fluctuations identified in Table II are indicated. Note that data was actually taken at 107 keV (c.m.) intervals only in the region from 20.5–22.5 MeV. Alternate data points are interpolated in other regions, owing to the requirements of the analysis programs. Analyses made with the original data set at intervals of 214 keV (c.m.) showed no profound differences from that illustrated here.

TABLE II. Effective number of channels contributing to the production of a given nuclide ($E_{c.m.}$ = 17–28 MeV).

Nuclide	$S(0)$	N_i	Nuclide	$S(0)$	N_i
Total fusion	1.7×10^{-4}	5700	^{24}Mg	1.5×10^{-3}	650 [a]
^{16}O	1.1×10^{-2}	95	^{25}Mg	5.6×10^{-3}	180
^{20}Ne	2.5×10^{-4}	3900 [b]	^{26}Mg	3.4×10^{-4}	2800
^{23}Na	2.0×10^{-4}	4800	^{26}Al	9.1×10^{-4}	1000
^{23}Mg	8.0×10^{-4}	1200	^{27}Al	8.4×10^{-3}	120

[a] Compare to an estimated value $N_i \sim 1400$ at $E_{c.m.} = 14.7$ MeV (Ref. 14).
[b] Compare to an estimated value $N_i \sim 5000$ at $E_{c.m.} = 16.7$ MeV (Ref. 14).

In the present case, we find that an averaging interval of 1.18 MeV (c.m.) is large enough to define a meaningful average cross section, but small enough to follow the gross structure evident in the data (Fig. 8).

A. Autocorrelation analysis

The autocorrelation function of the total fusion data is shown in Fig. 9. The most striking feature of this result is the existence of regular oscillations in $S(\epsilon)$ which persist to very large values of ϵ. The periodicity of ~725 keV is maintained with no evident reduction in amplitude to ϵ values >6 MeV in Fig. 9. Although finite-range-of-data (f.r.d.) effects are known to cause oscillations in $S_{\alpha\alpha}(\epsilon)$ for large values of ϵ, they are characterized by a period of about 2Γ (where Γ, the coherence width, is the width-at-half-maximum of the autocorrelation, equal to ~150–200 keV in this case). Furthermore, the amplitude of f.r.d. oscillations is expected to be substantially smaller than that of the observed periodic structure,[26] and the 725-keV periodicity is directly observable either in the deviation of the total fusion data from the local average (Fig. 10) or in the data itself (Fig. 5).

The next question to be answered, then, is whether these structures, despite their apparent regularity, are attributable to statistical fluctuations. This question can be answered in the context of standard Ericson theory[27] under the assumption that the direct-reaction contribution to these data is negligible. We begin by deducing the effective number of independent channels N_i contributing to each production cross section which, apart for a small correction factor[28] for f.r.d. effects, is simply the reciprocal of the autocorrelation function at $\epsilon = 0$ (Table II). The distribution of deviations $Z = \sigma(\epsilon)/\langle\sigma(\epsilon)\rangle$ from the mean cross section is given by a χ^2 distribution of $2N_i$ degrees of freedom,[27] which reduces to a Gaussian with standard deviation $\sigma = \sqrt{N_i}$ for $N_i \gtrsim 25$. The actual and expected distributions are shown in Figs. 11 and 12. It can be seen that, apart from the case of ^{24}Mg which will be discussed in more detail below, the deviations are rather well reproduced (as might be expected since the N_i have been deduced from experimental deviations). Nevertheless, there are indications of nonstatistical (or rather non-Ericson-fluctuation) components in the data. For example, the incidence of very large deviations is greater than expected from pure statistics. Furthermore, the calculated number of independent channels contributing to the total fusion yield is not simply the sum of N_i over all contributing nuclides, as it would be in pure Ericson theory, which suggests that there are many correlated channels. Finally, a Hauser-Feshbach calculation of the ^{12}C (^{16}O, α)^{24}Mg reaction[14,19] gives $N_i \approx 1400$ at $E_{c.m.} = 14.7$ MeV. Since N_i is expected to increase with increasing c.m. energy, the value $N_i = 650$ in Table II is clearly too small. In fact, $N_i = 1400$ gives a better fit to the observed distribution in its central region (Fig. 12). Thus, we conclude that $S(0)$ is being influenced by nonstatistical fluctuations, at least for ^{24}Mg.

Fortunately, the fact that our data contain production cross sections for several nuclides allows us to arrive at a more quantitative estimate of the contribution of nonstatistical fluctuations. In standard Ericson theory, these excitation functions are statistically independent data sets. Thus, we may look for "large" fluctuations which are correlated in several channels, using the predicted distributions of Figs. 11 and 12 to estimate the probability $P_i(E)$ that the observed deviation at a given c.m. energy is a statistical fluctuation. Such an analysis is given in Table III, in which we list, for each excitation function, the probability $P_i(E)$ for nine "independent" channels, as well as the total number of events $\langle N\rangle$ in the entire range of observation which would be expected, on the basis of pure statistics, to have the given signature (the nine values of P_i listed). Also given in Table III is the total number of expected events $\langle M\rangle$ based on the eight *least significant*

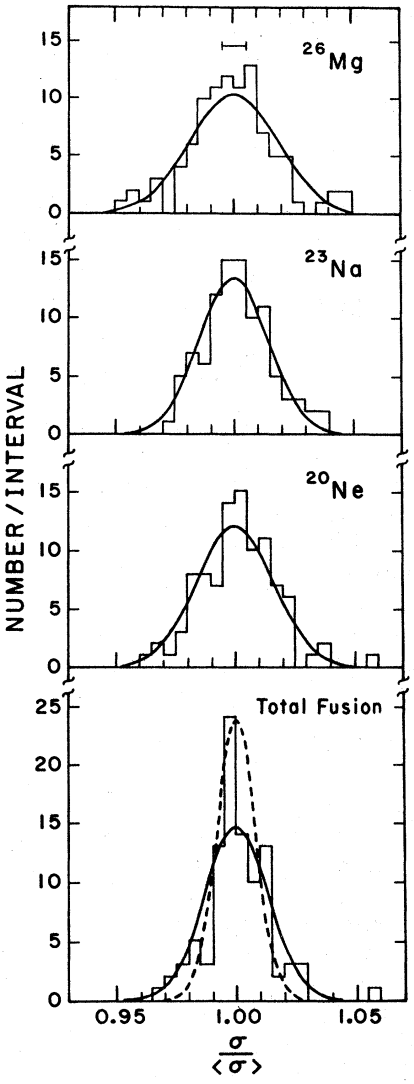

FIG. 11. Histograms of the deviations of various production cross sections from their local average values. The solid curve is a prediction derived from the autocorrelation function as discussed in the text. The dotted curve is a prediction for the total fusion cross section assuming that it is the incoherent sum of the individual evaporation channels. The error bar gives an estimate of the contribution from relative normalization uncertainties.

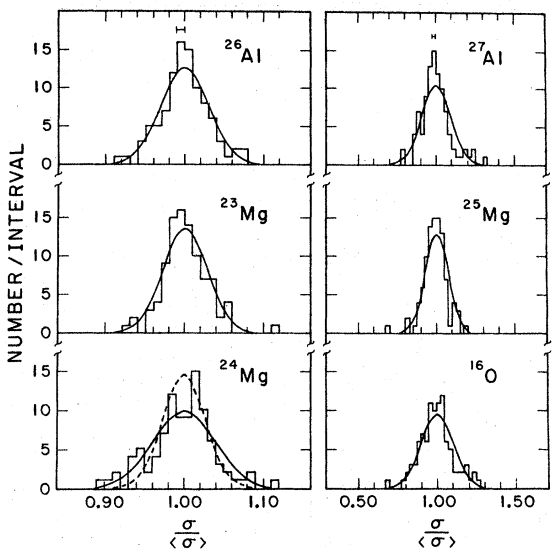

FIG. 12. Histograms of the deviations of various production cross sections from their local average values. See also Fig. 11 caption. The dotted curve gives prediction for ^{24}Mg based on an estimate of 1400 independent contributing channels.

excitation functions. Thus, a comparison of $\langle M\rangle$ and $\langle N\rangle$ gives a measure of the extent to which the signature of a given fluctuation depends on a single datum. We have included in Table III only those anomalies which have $\langle N\rangle$ values less than 10^{-2}, or have strong support from independent experiments. Certain anomalies also have $\langle M\rangle$ values less than 10^{-2}, and we indicate each of these cases with an asterisk in Table III, to indicate that it is extremely unlikely that such events are Ericson fluctuations. Note that, in assessing the significance of the $P_i(\epsilon)$ values, it should be kept in mind that they have been calculated using the N_i values of Table II (except for ^{24}Mg, for which we used the "better" value $N_i = 1400$). The presence of nonstatistical fluctuations in the data causes these N_i values to be systematically *underestimated*, resulting in an *overestimation* of $P_i(E)$. Thus, the actual probability that a given anomaly in Table III is an Ericson fluctuation will always be less (and sometimes substantially less) than that listed.

Referring now to Fig. 10, we note that all but three of the maxima and minima in the deviations of σ_{fus} from its local average are associated with anomalous (i.e., non-Ericson-fluctuation) structures in Table III. Since it is these extrema which produce the periodic modulation of $S(\epsilon)$ visible in Fig. 9, it is clear that the observed oscillations are not attributable to chance. However, the interpretation of these structures is also not self-evident. More than fifteen years ago, Temmer[29] predicted that regular oscillations might appear in heavy-ion reaction cross sections due to a resonant α-transfer mechanism. The $^{12}C + ^{16}O$ system is particularly suited for such a mechanism, as suggested by von Oertzen.[30] On the other hand, Matsuse, Abe, and Kondo[31] have recently calculated the total fusion cross section for $^{16}O + ^{12}C$ on the basis of a model involving the coupling of the 2^+ first excited state of ^{12}C to the elastic channel. They predict structure with a periodicity

TABLE III. Signatures of anomalous events in the excitation functions for $^{16}O + ^{12}C$.

$E_{c.m.}$ [a]	^{16}O	^{20}Ne	^{23}Na	^{23}Mg	^{24}Mg	^{25}Mg	^{26}Mg	^{26}Al	^{27}Al	$\langle N \rangle$ [b]	$\langle M \rangle$ [b]	Refs. [c]
17.71	+0.064	+0.016	+0.078	−0.30	+0.24	−6.4(5)	+0.63	−0.96	−0.96	1.6(8)	2.5(4)	d, e, *
18.14	+0.22	+0.14	+0.13	−0.88	+0.070	+0.52	+0.65	+0.56	+0.66	2.3(3)	0.032	f, g
18.57	+0.012	−0.028	−0.14	+0.76	−0.016	+0.66	−0.85	−0.96	−0.74	1.7(5)	1.4(3)	e, *
19.00	−0.001	+0.22	−0.74	−0.10	+0.74	−0.56	+0.94	+0.36	−0.72	1.7(4)	0.12	d
19.43	+0.032	−0.13	+0.44	+0.40	−0.12	−0.84	+0.71	+0.64	+0.48	1.2(3)	0.037	d
19.65	+0.018	−0.50	−0.86	−0.98	+0.15	−0.064	−0.92	−0.068	+0.26	8.8(5)	4.8(3)	h, i, d, g, *
19.86	−0.26	+0.046	−0.046	+0.24	−0.50	+0.66	+0.62	+0.092	+0.94	1.7(4)	3.8(3)	h, i, d, g, *
20.07	−0.40	−0.24	+0.15	+0.24	+0.032	+0.048	−0.11	−0.74	−0.84	2.8(5)	8.8(4)	*
20.72	+0.80	+0.006	+0.010	+0.44	+1.8(5)	+0.50	−0.98	+0.042	+0.11	6.4(11)	3.7(6)	j, d, f, *
20.93	+0.52	+0.96	+0.31	−0.94	−0.80	+0.11	+0.009	−0.019	−0.026	4.1(6)	4.8(4)	*
21.15	−0.30	−0.28	−0.12	−0.70	−0.010	−0.34	−0.57	−0.22	−0.50	1.1(4)	0.011	
21.47	+0.64	+0.22	+0.016	−0.94	+0.002	−0.019	−0.019	+0.26	−0.17	5.0(9)	2.5(6)	*
21.79	+0.40	−0.22	−0.28	−0.50	−0.003	+0.044	−0.60	+0.82	−0.46	2.6(5)	9.2(3)	d, *
(22.11)	−0.14	+0.16	+0.24	−0.94	+1.0	−0.72	+0.71	−0.90	−0.72	0.12	0.88	(j), d
22.43	+0.054	−0.68	+0.88	−0.48	−0.36	+0.48	+0.036	−0.90	+0.76	5.1(3)	0.14	(j)
(22.65)	+0.19	+0.78	−0.48	+0.38	+0.70	−0.64	+0.69	−0.14	−0.74	6.6(2)	0.46	d
22.86	−0.11	+0.17	+0.088	−0.90	+0.42	+0.60	+0.58	+0.26	+0.84	3.5(3)	0.041	j
(23.62)	+0.82	−0.22	−0.68	−0.72	−0.024	−0.38	+0.87	−0.56	+0.60	0.018	0.74	k
23.94	+0.20	−0.34	−0.38	+0.94	−0.30	−0.62	+0.89	+0.016	+0.88	4.3(3)	0.26	(j), (d)
24.37	−0.88	+0.26	+0.66	+0.086	+0.008	−0.54	+0.16	−0.096	+0.56	3.6(5)	4.6(3)	*
24.58	−0.50	−0.58	+0.064	−0.013	−0.38	−0.50	−0.50	−0.28	−0.17	7.8(5)	0.013	k
25.01	+0.68	−0.16	−0.60	+5.4(3)	+0.50	+0.44	+0.011	+0.036	+0.007	1.5(8)	6.3(6)	(j), *
25.22	+0.81	+0.80	+0.25	−7.1(3)	+0.33	−0.80	−0.012	−0.35	+0.97	9.1(5)	0.011	k
25.44	−0.48	−0.80	+0.78	−0.68	−3.8(4)	−0.38	+0.78	−0.60	+0.28	2.8(4)	0.78	l
(25.87)	+0.96	+0.68	+0.060	+0.82	+0.60	+0.72	+0.28	+0.30	−0.54	0.048	0.77	(j), l
26.30	−0.64	+1.0	−0.78	−0.54	+0.082	−0.66	+0.024	−0.063	+0.95	1.6(3)	0.064	(j), l
26.51	+1.0	+0.78	+0.52	−0.62	+0.002	+0.64	−0.078	+0.008	−0.34	4.8(6)	2.6(3)	*
26.94	+0.57	−0.79	−0.73	−0.56	−1.1(4)	−0.84	−0.017	+0.93	−0.13	2.5(6)	0.024	k
27.16	+0.90	+0.28	−0.50	+0.054	−0.84	−0.96	+0.53	+0.60	+0.001	1.7(4)	0.13	

[a] Energy of the anomaly. Parentheses indicate events which are listed only because of confirming evidence in other experiments. Plus or minus sign in signature indicates a deviation above or below $\langle \sigma \rangle$.

[b] Number in parentheses is the negative of the exponent. E.g., $1.6(8) = 1.6 \times 10^{-8}$.

[c] Letters in parentheses indicate tentative associations with anomalies observed in previous experiments. Asterisk indicates event with a very low probability of being an Ericson fluctuation, as determined in the present experiment (see text).

[d] R. E. Malmin, J. W. Harris, and P. Paul, Phys. Rev. C 18, 163 (1978).

[e] Reference 14.

[f] D. Branford, J. O. Newton, J. M. Robinson, and B. N. Nagorka, J. Phys. A 7, 1193 (1974).

[g] E. R. Cosman, A. Sperduto, T. M. Cormier, T. N. Chin, H. E. Wegner, M. J. LeVine, and D. Schwalm, Phys. Rev. Lett. 29, 1341 (1972).

[h] D. R. James, G. R. Morgan, N. R. Fletcher, and M. B. Greenfield, Nucl. Phys. A274, 177 (1976).

[i] R. E. Malmin, R. H. Siemssen, D. A. Sink, and P. P. Singh, Phys. Rev. Lett. 28, 1590 (1972).

[j] Reference 6.

[k] Reference 33.

[l] D. Shapira, R. M. DeVries, M. R. Clover, R. N. Boyd, and R. N. Cherry, Jr., Phys. Rev. Lett. 40, 371 (1978).

of 1.2 MeV, compared to the 725-keV periodicity of Fig. 9. Finally, it must be mentioned that similar oscillations have been observed in other reactions leading to the ^{28}Si compound nucleus,[32] so that it is possible that these structures are associated with properties of the ^{28}Si level densities, rather than with the $^{16}O + ^{12}C$ reaction mechanism itself.

B. Cross-correlation analysis

We define the reduced cross-correlation coefficient

$$R_{\alpha\alpha'}(\epsilon) = \frac{S_{\alpha\alpha'}(\epsilon)}{[S_{\alpha\alpha}(\epsilon) S_{\alpha'\alpha'}(\epsilon)]^{1/2}}, \tag{5}$$

such that $R(\epsilon)$ is unity for perfect functional re-

TABLE IV. Reduced cross-correlation coefficients $R(0)$. Errors (in parentheses) are dominated by f.r.d. effects. Diagonal elements are the autocorrelation coefficients $S(0)$ times 10^4.

	σ_{fus}	^{16}O	^{20}Ne	^{23}Na	^{23}Mg	^{24}Mg	^{25}Mg	^{26}Mg	^{26}Al	^{27}Al
σ_{fus}	1.7(0.3)	−0.20 (0.12)	0.91(0.17)	0.53(0.15)	0.26(0.13)	0.69(0.16)	−0.09 (0.14)	0.24(0.13)	0.43(0.14)	0.35 (0.14)
^{16}O		106 (19)	−0.27(0.14)	−0.17(0.14)	0.07(0.14)	−0.12(0.13)	−0.08 (0.14)	0.17(0.13)	−0.03(0.14)	0.03 (0.14)
^{20}Ne			2.5 (0.4)	0.34(0.14)	0.21(0.14)	0.50(0.14)	−0.17 (0.13)	0.17(0.13)	0.33(0.14)	0.27 (0.14)
^{23}Na				2.0 (0.4)	−0.13(0.14)	0.34(0.14)	−0.14 (0.14)	0.01(0.14)	0 (0.13)	−0.07 (0.13)
^{23}Mg					8.0 (0.14)	0.07(0.14)	0.45 (0.14)	0.26(0.13)	0.23(0.13)	0.36 (0.14)
^{24}Mg						15.3 (2.3)	−0.06 (0.13)	0.13(0.14)	0.16(0.13)	0.07 (0.14)
^{25}Mg							56 (10)	0.01(0.14)	0.08(0.14)	0.01 (0.13)
^{26}Mg								3.4 (0.6)	0 (0.13)	0.09 (0.13)
^{26}Al									9.1 (1.6)	0.31 (0.14)
^{27}Al										84 (15)

lationship between two excitation functions. The values of $R_{\alpha\alpha'}(0)$ deduced from the present data set are given in Table IV, where the indicated errors are dominated by f.r.d. effects[28] and are likely to be overestimated due to the method of obtaining N_i as discussed above. It can be seen that there are many statistically significant cross correlations, as might be expected from the discussion in the previous section. The extremely strong ^{20}Ne-σ_{fus} correlation is expected, simply because ^{20}Ne accounts for almost $\frac{1}{2}$ of σ_{fus} at all energies. On the other hand, the very strong correlations of ^{23}Na, ^{24}Mg, and ^{26}Al with σ_{fus}, and also the ^{20}Ne-^{24}Mg and ^{23}Mg-^{25}Mg cross correlations, are especially noteworthy since they exceed three-standard-deviation (99.7%) significance. Here, again, we have strong evidence for nonstatistical effects in the $^{16}O + ^{12}C$ reaction cross sections. Note also that the estimated ~10% contamination of the ^{20}Ne excitation function with a ^{23}Na γ ray (see above) will not substantially affect the fluctuation analysis since the two channels are seen to be strongly correlated.

It can be seen that all significant cross correlations in Table IV are positive, except for the ^{16}O-^{20}Ne (and ^{16}O-σ_{fus}) channels, which appear to be anticorrelated. This anticorrelation, which can be observed directly in Fig. 5, provided the impetus for the cross-correlation analysis presented here. In Fig. 13, we illustrate $S_{\alpha\alpha'}(\epsilon)$ for the ^{16}O-^{20}Ne correlation, demonstrating the strong oscillations which appear here as well as in the individual autocorrelation functions. Evidently, a nearly constant phase relationship between these two channels is maintained over 6 MeV c.m. energy.

These observations, together with the earlier

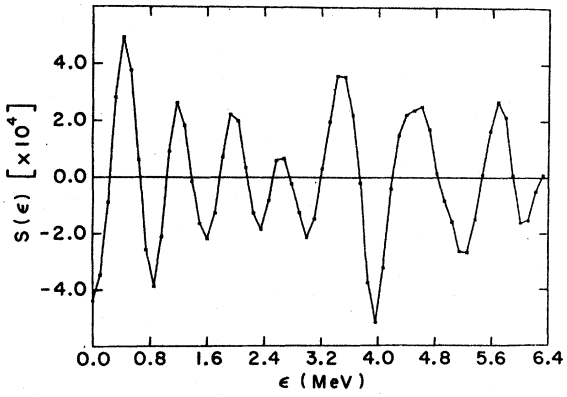

FIG. 13. Cross correlation function for the ^{16}O and ^{20}Ne excitation functions. Note the anticorrelation at $\epsilon = 0$, as well as the oscillatory behavior which is orthogonal to that shown in Fig. 9. Traces of the gross-modulation periodicity (~2.25 MeV) are also visible.

results of Katori, Furuno, and Ooi[33] and Malmin, Kahn, and Paul[34] on the reduced widths for resonances in $^{12}C + ^{16}O$ inelastic scattering, suggest a schematic model in which the inelastic-scattering and fusion channels are "coupled" by unitarity. In other words, it is possible that the observed oscillations in σ_{fus} are, to some extent, compensated for by the strong inelastic-scattering channels, so that the total *reaction* cross section is a smoothly varying function of energy as predicted by the optical model. Thus, the explanation of the narrow resonances in σ_{fus} is reduced to the task of explaining the inelastic resonances. This procedure corresponds to that followed by Matsuse, Abe, and Kondo.[31]

VI. CONCLUSION

The γ-ray yields from $^{12}C(^{16}O, x)$ reactions have been studied in the energy range from 17–28 MeV (c.m.). Ground-state transitions in 11 reaction residues were analyzed to give partial production cross sections. These were summed to obtain an excitation function for total fusion, which was found[7] to exhibit gross structure correlated with similar features in $^{12}C + ^{16}O$ inelastic scattering.[24] When corrected for the production of ^{16}O due to 3α evaporation, the fusion yield (averaged over the oscillations) was found to be essentially constant at 1 barn from 20–26 MeV (c.m.).

The partial production cross sections were used to deduce an "effective" α-particle yield to compare to the measured[15] α-particle production cross section. The agreement was found to be uniformly excellent over the entire data range up to 26 MeV (c.m.). This observation places severe constraints on possible mechanisms which can be invoked to explain disagreements between γ-ray[7, 13, 14] and heavy-ion detection[5] measurements in the region below 19 MeV (c.m.).

An evaporation-model calculation of the yield of reaction residues was not completely successful in reproducing the observed excitation functions. On the other hand, there were strong similarities between experiment and prediction for many of the channels, and the remaining discrepancies can be qualitatively understood as being due to an inappropriate approximation in the Hauser-Feshbach calculation. Thus, we conclude that there is no evidence that standard statistical models are inadequate to predict the average behavior of partial cross sections in this reaction.

The most striking result of the present experiment is the observation of narrow, regular fluctuations in the total fusion yield, with an average width of 150–200 keV (i.e., approximately one to three times that of compound-nuclear states at this excitation in ^{28}Si) and a periodicity of ~725 keV. Standard analysis of these anomalies shows conclusively that they are not Ericson fluctuations. Although questions can be raised[18] as to the applicability of Ericson theory in this region of excitation energy in ^{28}Si (and in particular, we have not attempted an R-matrix analysis of the data[35]), it seems likely that the explanation of the obvious regularities in the data (Fig. 9) will be of some interest.

Finally, we have demonstrated that many of the individual excitation functions discussed here are strongly correlated. One remarkable exception is the ^{16}O-^{20}Ne cross correlation, which shows clear evidence for anticorrelation. It is possible that this observation provides another link between inelastic-scattering and "fusion" resonances, along the lines suggested in the work of Matsuse, Abe, and Kondo.[31]

ACKNOWLEDGMENTS

The authors would like to thank Dr. R. E. Malmin for illuminating discussions concerning the fluctuation analysis, and for making his computer codes available to them. Thanks are also due to Dr. Jorge Gomez del Campo for granting permission to use his evaporation code. One of us (J. J. K.) would like to thank Brookhaven National Laboratory, where some of the preliminary analysis of the data was accomplished. This work was supported in part by the U. S. National Science Foundation.

[1] T. M. Cormier, C. M. Jachcinski, G. M. Berkowitz, P. Braun-Munzinger, P. M. Cormier, M. Gai, J. W. Harris, J. Barrette, and H. E. Wegner, Phys. Rev. Lett. 40, 924 (1978).
[2] P. Braun-Munzinger, G. M. Berkowitz, T. M. Cormier, C. M. Jachcinski, J. W. Harris, J. Barrette, and M. J. Levine, Phys. Rev. Lett. 38, 944 (1977).
[3] A. M. Sandorfi and A. M. Nathan, Phys. Rev. Lett. 40, 1252 (1978).
[4] A. J. Lazzarini, E. R. Cosman, A. Sperduto, S. G. Steadman, W. Thoms, and G. R. Young, Phys. Rev. Lett. 40, 1426 (1978).
[5] P. Sperr, S. Vigdor, Y. Eisen, W. Henning, D. G. Kovar, T. R. Ophel, and B. Zeidman, Phys. Rev. Lett. 36, 405 (1976).
[6] P. Charles, F. Auger, I. Badawy, B. Berthier, M. Dost, J. Gastebois, B. Fernandez, S. M. Lee, and E. Plagnol, Phys. Lett. 62B, 289 (1976).
[7] J. J. Kolata, R. M. Freeman, F. Haas, B. Heusch, and A. Gallmann, Phys. Lett. 65B, 333 (1976).
[8] R. J. deMeijer, A. G. Drentje, and H. S. Plendl, At. Data Nucl. Data Tables 15, 391 (1975).

[9]R. J. deMeijer and H. S. Plendl, At. Data Nucl. Data Tables 13, 1 (1974).
[10]P. M. Endt and C. Van Der Leun, Nucl. Phys. A214, 1 (1973).
[11]G. A. P. Engelbertink, L. P. Ekstrom, D. E. C. Scherpenzeel, and H. H. Eggenhuisen, Nucl. Instrum. Methods 143, 161 (1977).
[12]Data available in tabular form from one of the authors (J. J. K.).
[13]Z. E. Switkowski, H. Winkler, and P. R. Christensen, Phys. Rev. C 15, 449 (1977).
[14]D. Branford, B. N. Nagorcka, and J. O. Newton, J. Phys. G3, 1565 (1977).
[15]S. L. Tabor, Y. Eisen, D. G. Kovar, and Z. Vager, Phys. Rev. C 16, 673 (1977).
[16]A. Weidinger, F. Busch, G. Gaul, W. Trautmann, and W. Zipper, Nucl. Phys. A263, 511 (1976).
[17]LILITA, a Monte-Carlo, Hauser-Feshbach Computer Code, by J. Gomez del Campo and R. G. Stokstad, Oak Ridge National Laboratory (unpublished).
[18]R. E. Malmin, Argonne Physics Division Informal Report No. PHY-1972F (unpublished).
[19]L. R. Greenwood, K. Katori, R. E. Malmin, T. H. Braid, J. C. Stolzfus, and R. H. Siemssen, Phys. Rev. C 6, 2112 (1972).
[20]P. Sperr, T. H. Braid, Y. Eisen, D. G. Kovar, F. W. Prosser, Jr., J. P. Schiffer, S. L. Tabor, and S. Vigdor, Phys. Rev. Lett. 37, 321 (1976).
[21]See Ref. 16 for a discussion of the sensitivity of these calculations to particular parameters of the theory.
[22]A. Gilbert and A. G. W. Cameron, Can. J. Phys. 43, 1446 (1965).
[23]J. J. Kolata, R. M. Freeman, F. Haas, B. Heusch, and A. Gallmann (unpublished).
[24]C. M. Jachcinski, T. M. Cormier, P. Braun-Munzinger, G. M. Berkowitz, P. M. Cormier, M. Gai, and J. W. Harris, Phys. Rev. C 17, 1263 (1978).
[25]G. Pappalardo, Phys. Lett. 13, 320 (1964).
[26]W. R. Gibbs, Los Alamos Report No. LA-3266, 1965 (unpublished).
[27]T. Ericson, Ann. Phys. (N.Y.) 23, 390 (1963).
[28]P. J. Dallimore and I. Hall, Nucl. Phys. 88, 193 (1966).
[29]G. M. Temmer, Phys. Lett. 1, 10 (1962); this model is further developed by G. Michaud and E. W. Vogt, Phys. Lett. 30B, 85 (1969); Phys. Rev. C 5, 350 (1972).
[30]W. von Oertzen, Nucl. Phys. A148, 529 (1970).
[31]T. Matsuse, Y. Abe, and Y. Kondo, Prog. Theor. Phys. 59, 1037 (1978).
[32]P. P. Singh, R. E. Segel, L. Meyer-Schützmeister, S. S. Hanna, and R. G. Allas, Nucl. Phys. 65, 577 (1965); R. V. Elliot and R. H. Spear, Nucl. Phys. 84, 209 (1966); L. W. Put, J. D. A. Roeders, and A. Van Der Woude, *ibid.* A112, 561 (1968).
[33]K. Katori, K. Furuno, and T. Ooi, Phys. Rev. Lett. 40, 1489 (1978).
[34]R. E. Malmin, F. Kahn, and P. Paul, Phys. Rev. C 17, 2097 (1978).
[35]P. A. Moldauer, Phys. Rev. Lett. 18, 249 (1967); Phys. Lett. 8, 70 (1964).